Synthesis, X-ray Structures, Spectroscopic and Thermal Characterization of Two New Organic Ammonium Tetrathiotungstates

Bikshandarkoil R. Srinivasan[a], Sunder N. Dhuri[a], Martha Poisot[b], Christian Näther[b], and Wolfgang Bensch [b,*]

[a] Goa/India, Department of Chemistry, Goa University
[b] Kiel, Institut für Anorganische Chemie der Christian-Albrechts Universität

Received December 6th, 2004.

Dedicated to Professor Rüdiger Kniep on the Occasion of his 60th Birthday

Abstract. Two new tetrathiotungstates ($pipH_2$)[WS_4] (**1**) and ($trenH_2$)[WS_4] · H_2O (**2**) (pip = piperazine and tren = tris(2-aminoethyl)amine) were synthesized and characterized by elemental analysis, infrared, Raman, UV-Visible and ^{1}H NMR spectroscopy, single crystal X-ray crystallography, and thermoanalysis. In **1** and **2** the amines pip and tren are diprotonated and they are linked to the $[WS_4]^{2-}$ tetrahedra via weak N-H···S (**1**, **2**) and N-H···O (**2**) hydrogen bonds. In **2** the H atoms of the H_2O molecule have also contacts to S atoms. The strength and number of the S···H interactions affect the W-S bond lengths and a relatively long W-S bond of 2.2147(7) Å is observed in **1** while the longest W-S bond in **2** is 2.1997(6) Å. The different degree of distortion of the $[WS_4]^{2-}$ anions is reflected in the IR and Raman spectra. The compounds decompose upon heating in an inert atmosphere to form amorphous $WS_{2.1}C_{1.2}N_{0.3}$ and $WS_{2.1}C_3N_{0.8}$ respectively, and the C and N content of the decomposition products is determined by the C and N content of the amines. In contrast to other tetrathiotungstates, the thermal reaction of both compounds do not proceed via amorphous WS_3 as an intermediate phase. Compound **2** can be reversibly de- and re-hydrated, and the process of re-hydration proceeds presumably via dissolution-re-crystallization mechanism.

Keywords: Tetrathiotungstates; Crystal structures; Spectral and Thermal Properties

Introduction

The chemistry of soluble metal sulfide complexes is still an attractive field of research due to its importance in hydrodesulfurization catalysis (HDS), environment and material science [1]. The soluble sulfides of the group VI metals W and Mo [2, 3] are unique as they exhibit a wide range of metal to sulfur stoichiometries, metal oxidation states, coordination and bonding modes of the sulfido ligands. Interestingly, many of the known W-S complexes have been synthesized using the simple mononuclear tetrathiotungstate indicating that $[WS_4]^{2-}$ is an useful starting material in W-S chemistry. The ammonium salt of tetrathiotungstate was first prepared a long time ago by *Berzelius* [4], but much of its chemistry has been developed only in the last three decades [5] since the first reported synthesis of $[Ni(WS_4)_2]^{2-}$ complex [6].

In recent years, the use of organic ammonium tetrathiotungstates as precursors for the preparation of WS_2 catalysts has shown much promise in the field of hydrodesulfurization (HDS) catalysis [7]. The nature of the organic moiety in the precursors has been shown to affect the surface area, pore size distribution, the carbon content as well as HDS selectivity. Interestingly, only few of these tetrathiotungstates have been structurally characterized. In addition, a systematic study how the organic ammonium species influences and determines the final carbon content has not been undertaken until now. The tetrahedral $[MS_4]^{2-}$ (M = W, Mo) unit is an important building block, which can be used to generate a great variety of fascinating structures [2, 3]. This structural diversity can be attributed to the flexibility of the tetrahedral motif as evidenced by the structural characterization of several $[WS_4]^{2-}$ and also the corresponding $[MoS_4]^{2-}$ complexes with several counter ions in our recent work [8–19]. In almost all these complexes, the $[MS_4]$ tetrahedron is slightly distorted with one or two of the M-S bonds elongated, which we have explained on the basis of the strength and numbers of S···H interactions between $[MS_4]^{2-}$ and the organic cation. It has also been reported in the literature for Mo-S compounds that the chemical properties of $[MoS_4]^{2-}$ can be substantially changed by surrounding it with bulky organic ammonium cations [20]. The role of hydrogen bonding interactions between the cation and anion to influence the reactivity characteristics has also been reported [21]. In view of this we are investigating the synthesis, structural and thermal characterization of organic ammonium tetrathiometalates of the group VI metals and have already shown that a rich chemistry of tetrathiomolybdates can be developed by suitably changing the hydrogen bonding interactions between the cation and $[MoS_4]^{2-}$ [22]. In continuation of this work, we describe herein the synthesis, spectroscopic, thermal and X-ray structural characterization of two new

* Prof. Dr. Wolfgang Bensch
Inst. f. Anorg. Chemie der Universität
Olshausenstr. 40
D-24098 Kiel
Fax: +49-(0)431-880-1520
E-mail: wbensch@ac.uni-kiel.de

Table 2 Hydrogen-bonding (in Å, °) for $(pipH_2)[WS_4]$ (**1**).

D-H···A	d(D-H)	d(H···A)	<DHA	d(D···A)	Symmetry code
N2-H1···S1	0.900	2.486	140.83	3.234	x−1, y, z
N2-H2···S1	0.900	2.458	163.71	3.331	x−1, −y+1/2, z−1/2
N1-H1···S2	0.900	2.389	166.67	3.272	
N1-H1···S2	0.900	2.587	138.85	3.318	x, −y+1/2, z−1/2
N2-H1···S3	0.900	2.881	124.33	3.470	x−1, y, z
N1-H2···S4	0.900	2.638	130.95	3.299	x, −y+1/2, z−1/2
N2-H2···S4	0.900	2.841	112.07	3.287	x−1, −y+1/2, z−1/2

tetrathiotungstates obtained by the reaction of $[WS_4]^{2-}$ with the cyclic diamine piperazine (pip) and the polyamine tris(2-aminoethylamine) (tren).

Results and Discussion

Crystal Structures

The synthesis of the two new tetrathiotungstates was readily accomplished in good yields by the base promoted cation exchange reaction. The details of this synthetic route have already been described in our recent report [22]. The compounds **1** and **2** are quite stable in air and less soluble in water unlike ammonium tetrathiotungstate. However, both are freely soluble in aqueous ammonia. In the structures of the title compounds tetrahedral $[WS_4]^{2-}$ anions and the counter cations $(pipH_2)^{2+}$ (in **1**), and $(trenH_2)^{2+}$ (in **2**) are found. In **1** and **2** all unique atoms are located on general positions. Compound **1** is isostructural to $(pipH_2)[MoS_4]$ recently reported by us [22]. In (**1**) the $(pipH_2)^{2+}$ cations and $[WS_4]^{2-}$ anions are connected via weak hydrogen bonds. The organic cation adopts the chair form with C-C and C-N bond lengths and bond angles being in good agreement with those for other complexes containing the same cation [22−24]. The $[WS_4]^{2-}$ tetrahedron is slightly distorted (S-W-S angles: 108.57(3)−110.49(3)°, Table 1). The W-S bonds vary from 2.1762(7) to 2.2147(7) Å, with a mean W-S bond length of 2.1937 Å (Table 1). These parameters agree well with those in other compounds like $[Ni(tren)_2][WS_4]$ [8] or $(enH_2)[WS_4]$ (en = ethylenediamine) [9]. Two W-S bonds are longer, while the other two are shorter at around 2.1762(7) Å. The elongation of W-S bond distances can be attributed to short S···H contacts (2.389 to 2.881 Å) (Table 2), which results in an extended three-dimensional hydrogen-bonded network (Fig. 1). The S···H distances in **1** are shorter than in $(enH_2)[WS_4]$ (2.432−3.003 Å). In **1** S(1), S(2), and S(4) have two S···H contacts while S(3) has only one (Table 3). This feature is responsible for the very short W-S(3) distance of 2.1762 (7) Å. The D-H···A bond angle of 124.33° together with the longest S···H distance of 2.881 Å observed for S(3) indicates a very weak interaction. The shortest S···H separation of 2.389 Å is accompanied by the largest D-H···A

Table 1 Selected bond lengths and angles (in Å, degree) for $(pipH_2)[WS_4]$ (**1**).

W(1)-S(3)	2.1762(7)	N(1)-C(4)	1.492(4)
W(1)-S(4)	2.1797(7)	C(1)-C(2)	1.510(4)
W(1)-S(1)	2.2042(7)	C(2)-N(2)	1.502(4)
W(1)-S(2)	2.2147(7)	N(2)-C(3)	1.479(4)
N(1)-C(1)	1.485(4)	C(3)-C(4)	1.510(3)
S(3)-W(1)-S(4)	110.49(3)	C(1)-N(1)-C(4)	111.6(2)
S(3)-W(1)-S(1)	109.67(3)	N(1)-C(1)-C(2)	110.7(2)
S(4)-W(1)-S(1)	108.57(3)	N(2)-C(2)-C(1)	110.0(2)
S(3)-W(1)-S(2)	110.12(3)	C(3)-N(2)-C(2)	112.1(2)
S(4)-W(1)-S(2)	108.75(3)	N(2)-C(3)-C(4)	110.3(2)
S(1)-W(1)-S(2)	109.20(3)	N(1)-C(4)-C(3)	110.3(2)

Table 3 Selected bond lengths and angles (in Å, degree) for $(trenH_2)[WS_4]\cdot H_2O$ (**2**).

W(1)-S(3)	2.1739(6)	C(1)-C(2)	1.512(3)
W(1)-S(1)	2.1925(7)	C(2)-N(2)	1.489(3)
W(1)-S(2)	2.1954(6)	C(3)-C(4)	1.505(3)
W(1)-S(4)	2.1997(6)	C(4)-N(3)	1.477(4)
N(1)-C(1)	1.470(3)	C(5)-C(6)	1.521(3)
N(1)-C(5)	1.471(3)	C(6)-N(4)	1.458(3)
N(1)-C(3)	1.475(3)		
S(3)-W(1)-S(1)	108.09(3)	C(5)-N(1)-C(3)	110.58(18)
S(3)-W(1)-S(2)	110.90(3)	N(1)-C(1)-C(2)	110.60(17)
S(1)-W(1)-S(2)	109.68(3)	N(2)-C(2)-C(1)	110.52(18)
S(3)-W(1)-S(4)	109.80(3)	N(1)-C(3)-C(4)	111.97(19)
S(1)-W(1)-S(4)	109.63(3)	N(3)-C(4)-C(3)	110.6(2)
S(2)-W(1)-S(4)	108.73(2)	N(1)-C(5)-C(6)	113.7(2)
C(1)-N(1)-C(5)	111.93(18)	N(4)-C(6)-C(5)	116.0(2)
C(1)-N(1)−C(3)	110.98(17)		

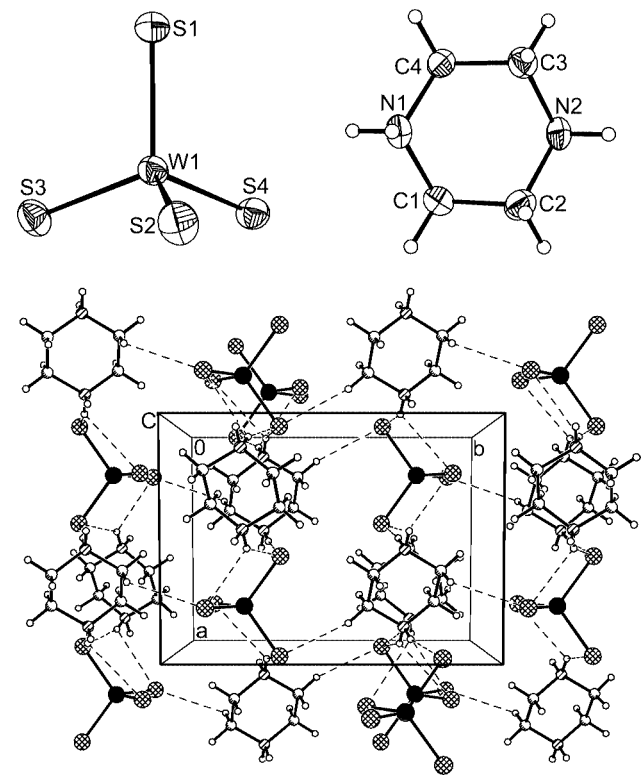

Fig. 1 Crystal structure of $(pipH_2)[WS_4]$ (**1**) with view of the $[WS_4]^{2-}$ anion (top: left) and the $(pipH_2)^{2+}$ cation (top: right) with labeling and displacement ellipsoids drawn at the 50 % probability level. The packing along the c-axis is shown in the lower part (hydrogen bonding is shown as dashed lines).

angle which can explain the long W-S(2) bond of 2.2147(7) Å. The intermediate W-S bond lengths can be similarly explained based on the strengths of the H-bonding interactions. To our knowledge, the W-S(2) distance of 2.2147(7) Å in **1** is one of the longest W-S bonds in tetrathiotungstates and is comparable with that in (1,4-dmpH$_2$)[WS$_4$] (1,4-dmpH$_2$: 1,4-dimethylpiperazinium) of 2.2136(8) Å [11]. In addition, in **1** the difference between the longest and the shortest W-S bonds of 0.0385 Å is large, and this probably is responsible for the appearance of a split W-S vibration in the IR spectrum.

Compound **2** is isostructural with (trenH$_2$)[MoS$_4$] · H$_2$O [22] containing the diprotonated (trenH$_2$)$^{2+}$ ion. In **2** (trenH$_2$)$^{2+}$cations, [WS$_4$]$^{2-}$ anions and H$_2$O molecules are present (Fig. 2). We note that **2** is the first example of a structurally characterized hydrated tetrathiotungstate. Interatomic distances and angles in (trenH$_2$)$^{2+}$ are in excellent agreement with those in [Co$_2$(tren)$_3$][MoS$_4$]$_2$ and (trenH$_2$)[MoS$_4$] · H$_2$O [15, 22]. The [WS$_4$]$^{2-}$ tetrahedron is slightly distorted with W-S bond lengths in the range of 2.1739(6) to 2.1997(6) Å (mean W-S distance: 2.1904 Å) (Table 3). Three of the W-S bonds are longer than the average W-S distance of 2.1893 Å reported for (enH$_2$)[WS$_4$] [9]. In **2** short S···H-N contacts are observed which are slightly longer than in **1** (Table 4 and Fig. 2). The shortest W-S bond of 2.1739(6) Å is observed for S(3), which has only

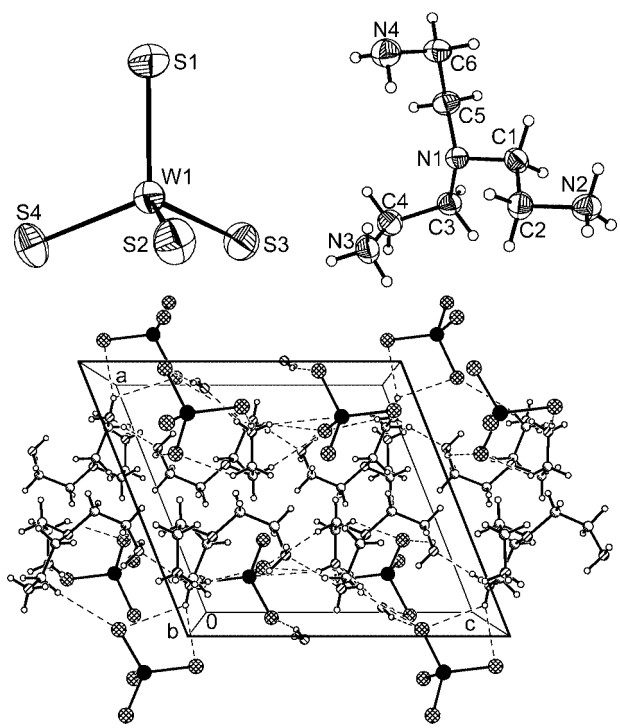

Fig. 2 Crystal structure of (trenH$_2$)[WS$_4$] · H$_2$O (**2**) with view of the WS$_4$ anion (top: left) and the (trenH$_2$)$^{2+}$ cation (top: right) with labeling and displacement ellipsoids drawn at the 50 % probability level and of the packing in the direction of the c-axis (bottom) (hydrogen bonding is shown as dashed lines).

Table 4 Hydrogen-bonding (in Å, °) for (trenH$_2$)[WS$_4$]·H$_2$O (**2**).

D-H···A	d(D-H)	d(H···A)	<DHA	d(D···A)	Symmetry code
N2-H1···S1	0.861	2.946	119.97	3.457	x+1, −y+1/2, z+1/2
N4-H2···S1	0.892	3.015	128.32	3.636	x+1, y, z
O1-H1···S1	0.822	2.500	161.20	3.289	x+1, y, z
O1-H2···S1	0.822	2.596	169.28	3.407	−x+1, y+1/2, −z+1/2
N2-H1···S2	0.861	2.590	158.17	3.405	x+1, −y+1/2, z+1/2
N2-H2···S2	0.862	2.994	110.07	3.388	−x+1, y−1/2, −z+1/2
N3-H3···S2	0.861	2.462	172.65	3.318	−x+1, y+1/2, −z+1/2
N4-H1···S3	0.891	2.939	148.28	3.727	−x+1, y+1/2, −z+1/2
N2-H2···S4	0.862	2.536	169.24	3.387	−x+1, y−1/2, −z+1/2
N3-H1···S4	0.862	2.634	152.95	3.424	−x+1, −y+1, −z+1
N2-H3···N4	0.862	1.946	176.84	2.807	x, −y+1/2, z+1/2
N3-H2···O1	0.862	1.983	156.99	2.797	

one contact to a H atom at a distance of 2.939 Å (Table 4). The analysis of the situation for S(1) and S(4) shows some interesting trends. S(4) has two contacts to H atoms of 2.536 and 2.634 Å, N-H···S(4) angles of 169.24 and 152.95° and the longest W-S bond length of 2.1997(6) Å. S(1) has two contacts to H atoms of the ammonium groups and two to H atoms of H$_2$O (Table 4). The two former are long (2.946 Å, 119.97°; 3.015 Å, 128.32°) while the latter two interactions are significantly shorter (2.500 Å, 161.20°; 2.596 Å, 169.28°). The W-S(1) bond of 2.1925(5) Å is surprisingly short as one would expect that this bond is at least as long as the W-S(4) bond. One possible explanation may be that despite the short S(1)···H distances to the H atoms of H$_2$O the interactions are weaker than those to H atoms bound to N. This explanation gains more credence as a similar behavior was observed in the isostructural Mo complex [22]. Finally, S(2) has two short contacts, and the W-S(2) bond amounts to 2.1954(6) Å. The difference between the longest and the shortest W-S bond distances in **2** of 0.0158 Å is smaller than that observed in **1**.

Spectral studies

The UV-Visible spectra of **1** and **2** in dilute aqueous ammonia exhibit bands at around 393, 277 and 221 nm. The peak positions are almost identical to that in the corresponding ammonium or tetraethylammonium salts [5, 25] and can be assigned to the charge transfer transitions of the tetrahedral [WS$_4$]$^{2-}$ moiety. The ^{1}H NMR spectrum of **1** in DMSO-d_6 exhibits a sharp singlet at δ = 3.25 ppm assignable to the magnetically equivalent methylene protons. Two triplets at δ = 2.55 (J = 6 Hz) and δ = 2.82 (J = 5.5 Hz) one each for the equivalent -CH$_2$ groups (C1, C3 and C5) directly bonded to N1 and the other for the remaining three -CH$_2$ groups (C2, C4 and C6) are observed in the ^{1}H NMR spectrum of **2**. Because only these signals are observed a very rapid exchange of the N-H protons with the trace amounts of water in DMSO-d_6 can be assumed.

The bands in the central part of the IR spectra of **1** (Fig. 3), and **2** (Fig. 4) are due to absorptions of the organic cations. The IR of **2** exhibits a broad and strong band at around 3471 cm^{-1} due to the O-H stretching vibration of H$_2$O. The N-H stretching modes appear at around

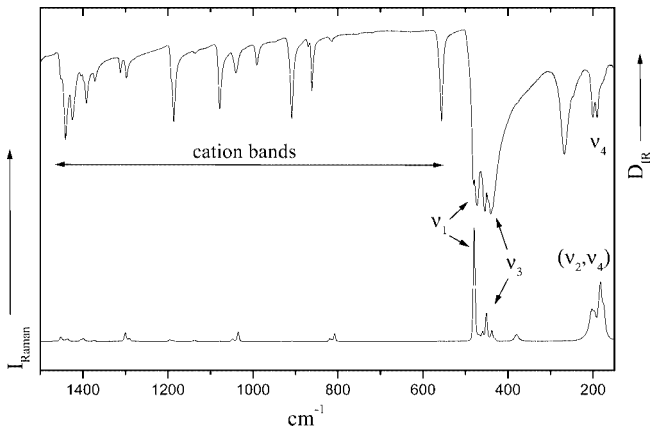

Fig. 3 Raman and IR spectra of $(pipH_2)[WS_4]$ (**1**).

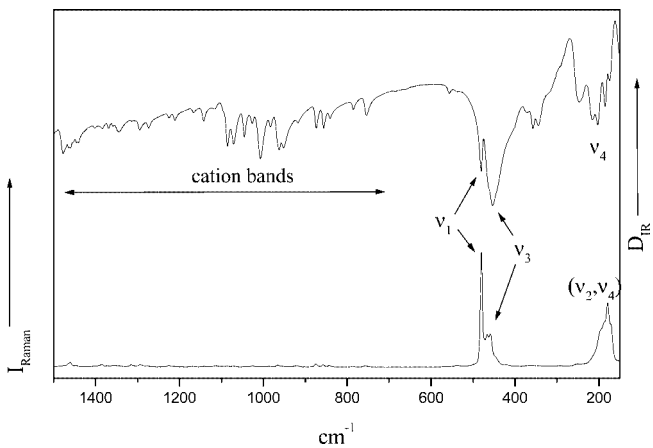

Fig. 4 Raman and IR spectra of $(trenH_2)[WS_4]\cdot H_2O$ (**2**).

3000 cm^{-1} in **1** and at 3084 and 3009 cm^{-1} in **2**. The shift to lower wave numbers compared to the free amines in **1** or **2** can be attributed to the H-bonding interactions (N-H···S). For free tetrahedral $[WS_4]^{2-}$ anions four characteristic bands $\nu_1(A_1)$, $\nu_2(E)$, $\nu_3(F_2)$, and $\nu_4(F_2)$ are expected [26]. All four bands are Raman active while only ν_3 and ν_4 are infrared active. Many tetrathiotungstates exhibit a single strong band at around 455 cm^{-1} assignable to the triply degenerate asymmetric stretching vibration (ν_3) of the W=S bond [5, 26]. Interestingly, for **1** ν_3 is split and appears as a doublet at 454 and 441 cm^{-1} with a further band around 473 cm^{-1} (Fig. 3). The observed extra signals cannot be caused by the $(pipH_2)^{2+}$ cations as no strong signals are observed for $(pipH_2)Cl_2$ below 500 cm^{-1}. Hence these features indicate considerable distortion of the $[WS_4]$ tetrahedron and can be explained by the lowering of symmetry [5], which is probably responsible for the symmetric stretching vibration (ν_1) of the W=S bond at 473 cm^{-1} to appear in the spectrum. The IR inactive (ν_1) vibration is normally not observed for undistorted tetrahedral compounds. The assignment of the 473 cm^{-1} band for the symmetric stretching vibration gains credence from the observation of an intense signal in the Raman spectrum at 480 cm^{-1}. The IR active (ν_4) vibration is also observed as a doublet at 191 and 201 cm^{-1}. The weak signal at 451 cm^{-1} in the Raman spectrum can be assigned to the (ν_3) vibration while the signal at 183 cm^{-1} is due to the degenerate (ν_2) and (ν_4) modes. For **2** the IR absorptions are observed at 481 and 454 cm^{-1}. Unlike in **1** the signal at 454 cm^{-1} is not clearly split even though it appears quite broad (Fig. 4), i. e. the distortion of the anion is less pronounced in accordance with the smaller difference in bond distances between the longest and the shortest W-S bonds. The IR spectrum of complex **2** can be explained similarly as for **1**.

Thermal studies

The thermal decomposition behavior of $(NH_4)_2[WS_4]$ is well documented and is represented by the equation (1)

$$(NH_4)_2[WS_4] \rightarrow 2\ NH_3 + H_2S + WS_3 \quad (1)$$

The compound is stable up to 180 °C and decomposes with an endothermic peak at 280 °C [5, 27]. The intermediate formed WS_3 has been reported to be stable between 310 and 340 °C followed by decomposition into S and WS_2. The formation of WS_2 is accompanied by a sharp exothermic event at 339 °C. Compound **1** is found to be thermally more stable and decomposition starts at 208 °C accompanied by a strong endothermic signal at T_{peak} = 289 °C (Fig. 5). We note that **1** is also thermally more stable than the corresponding isostructural Mo analog ($T_{decomp.}$ = 140 °C) [22]. Until 400 °C a mass loss of about 30 % is observed. Above 400 °C the weight change is small and the total loss till 600 °C is 32.14 %. For the formation of WS_3 the expected value is 30.04 % and for WS_2 38.04 %. Interestingly, after the heat treatment the residue contains 1.87 % N and 5.54 % C leading to a composition $WS_{2.1}C_{1.2}N_{0.3}$ (EDX:

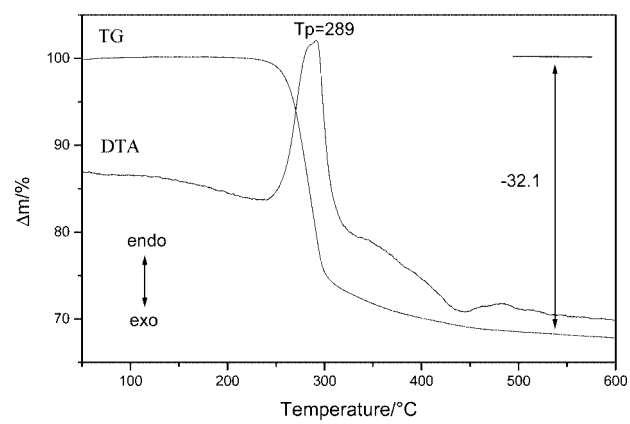

Fig. 5 DTA and TG curves for $(pipH_2)[WS_4]$ (**1**) (heating rate 4 K/min; N_2 atmosphere; given are the peak temperatures (T_p) in °C and the mass loss in %).

W:S = 1:1.94). In the X-ray powder pattern of the black decomposition product only broad modulations are observed, indicating that the material is amorphous. The formation of a predominantly disulfide residue by the thermal decomposition of **1** in a single endothermic step at a relatively low temperature indicates that in contrast to other tetrathiotungstates no WS_3 is formed as an intermediate.

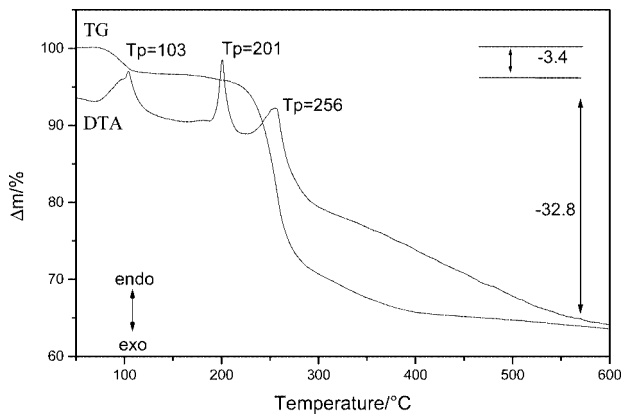

Fig. 6 DTA and TG curves for $(trenH_2)[WS_4]\cdot H_2O$ (**2**) (heating rate 4 K/min; N_2 atmosphere; given are the peak temperatures (T_p) in °C and the mass loss in %).

Compound **2** loses the water starting at about 70 °C ($-H_2O$ Δm_{exp} = 3.43 %; H_2O Δm_{theo} = 3.76 %) with T_{peak} = 103 °C (Fig. 6). Increasing the temperature two more endothermic events are observed with T_{peak} = 201 and 256 °C and a mass loss of 32.8 % is obtained. In another experiment the decomposition was stopped at about 110 °C and the anhydrous product thus obtained exhibited a significantly different X-ray powder pattern compared to that of the starting material. The second endothermic peak is not accompanied with a significant mass loss and therefore decomposition of the material was stopped at 210 °C in another experiment. Interestingly, in the crucible a black melt was formed and the X-ray powder pattern showed only a strong modulated background.

The thermal behavior of **2** is quite similar to that of $(trenH_2)[MoS_4]\cdot H_2O$ [22] with a slightly lower value for the dehydration process, while the decomposition of the anhydrous tetrathiotungstate thus formed is observed at elevated temperatures as compared to the Mo analogue. This observation is similar to that observed for complex **1** and indicates that $[WS_4]^{2-}$ complexes are thermally more stable than the corresponding $[MoS_4]^{2-}$ analogues. However, as for compound **1** the final black residue shows appreciable amounts of C (12.01 %) and N (3.67 %) yielding a composition $WS_{2.1}C_3N_{0.8}$. The presence of more C and N in the residue of **2** than in **1** is presumably due to the larger C and N content of tren compared to pip in **1**, indicating that a larger C content of the staring material yields a product containing more C. This observation is of special interest because for active HDS catalysts the actual C content is important. As for **1** the amorphous nature of the residue is evident in the X-ray powder diagram (not shown). In view of the emerging importance of disulfide materials as well as carbon contaminated metal sulfides in catalysis, additional experiments involving different heating rates and characterization of the intermediates formed are underway.

Re-hydration studies

Compound **2** emits water at a relatively low temperature. In further experiments the re-hydration behavior of the dehydrated sample was studied with X-ray diffractometry and electron microscopy. The dehydrated sample was stored in a desiccator over water atmosphere and powder patterns were collected after distinct times. The reaction is slow as can be seen in Fig. 7, and the dehydrated and re-hydrated phases coexist over a long time. After 6 days the pattern is very similar to that of the pristine compound. To gain further insight how the reaction takes place selected crystals were investigated after dehydration and after re-hydration (Fig. 8). As can be seen in Fig. 8 (top) the surface of the crystal after the heat treatment is relatively smooth with some small holes. After re-hydration the surface is rough with a large number of small cavities (Fig. 8, bottom). One possible explanation is that the dehydrated material partially dissolves in the water vapor and re-crystallizes forming the H_2O containing starting material, i.e. it is a dissolution-re-crystallization reaction. The process is slow explaining the long time until full re-hydration is observed.

Conclusions

Two new tetrathiotungstates $(pipH_2)[WS_4]$ (**1**) and $(trenH_2)[WS_4]\cdot H_2O$ (**2**) are obtained in good yields by the base promoted cation exchange method. Compound **2** is the first example of a structurally characterized hydrated tetrathiotungstate. In both compounds the $[WS_4]^{2-}$ tetra-

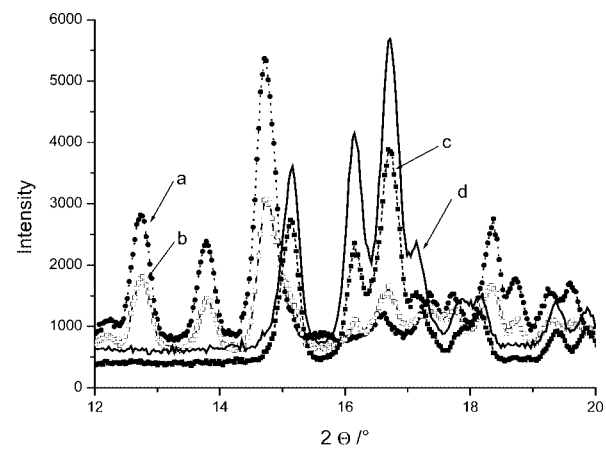

Fig. 7 X-ray powder patterns of dehydrated compound **2** (trace a), re-hydrated for 2 d (trace b), re-hydrated for 6 d (trace c), and the pristine material (trace d).

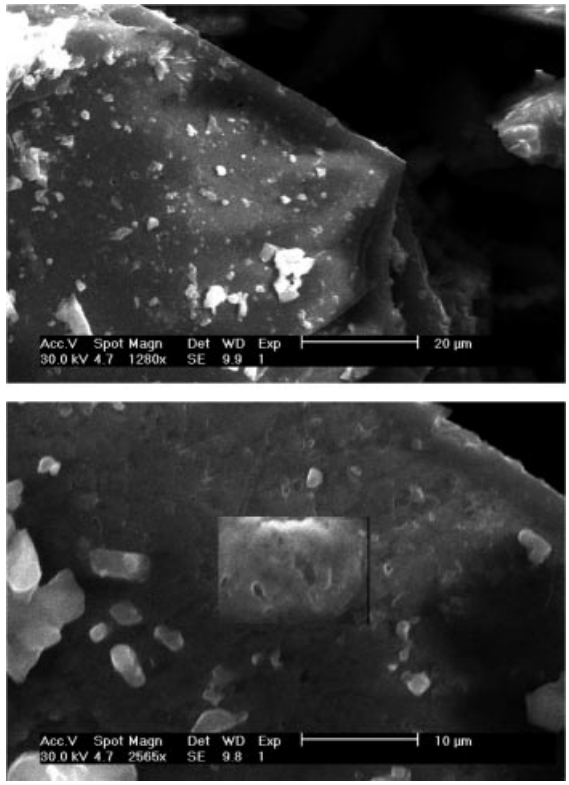

Fig. 8 SEM micrographs of **2** after dehydration (top) and after re-hydration (bottom).

hedra are distorted which can be explained on the basis of the strength and number of N-H···S interactions. In **2** N-H···S as well as O-H···S interactions are observed. The rigorous analysis of the geometric parameters in **2** suggests that the O-H···S interactions are weaker compared to the N-H···S interactions in terms of their ability to elongate W-S bonds. Our future work in this field is directed to the synthesis of new tetrathiotungstates which exhibit both types of such interactions. In addition, the results of the thermal decomposition reactions are of special interest for the preparation of C containing amorphous WS_2 materials as HDS catalysts which are obtained without the formation of a WS_3 intermediate, i.e. in the final amorphous products the W:S ratio is close to 1 : 2. Systematic experiments are also under way to correlate the residual C and N content in the WS_2 phases with the available C and N content in the starting tetrathiotungstates. The directed thermal decomposition of suitable R[WS_4] precursors (R = organic cation) can be a promising and easy route for the preparation of WS_2 based HDS catalysts.

Experimental Section

Materials and methods

The amines pip, tren, tungstic acid and the solvents were used in this investigation as obtained from commercial sources with analytical purity. $(NH_4)_2[WS_4]$ was prepared by literature method [25]. Far-IR spectra (range 80 to 500 cm^{-1}) were measured on a Bruker IFS 66 infrared spectrometer in pressed polyethylene disks. MIR spectra of the compounds were recorded in a KBr matrix. The samples were ground with dry KBr into fine powders and pressed into transparent pellets. The spectra were recorded in the IR region of 450-3000 cm^{-1}, (resolution 1 cm^{-1}) by an ATI Mattson Genesis infrared spectrometer. Raman spectra were measured in the region 100-3500 cm^{-1} on a Bruker FRA106 Fourier transform Raman spectrometer. ^1H NMR spectra were recorded on a Bruker 300 MHz FT-NMR instrument. UV-Visible spectra were recorded in dilute ammonia using matched quartz cuvettes on a Varian Cary 5 UV-VIS-NIR equipment. C, H, N and S analyses were performed on a HEKA Tech Euro EA elemental analyzer. DTA-TG measurements were performed simultaneously using a Netzsch STA-409CD device. The thermal investigations were performed in Al_2O_3 crucibles using a heating rate of 4 K/min up to 600 °C and purged in a nitrogen stream of 75 mL/min. EDX analysis was performed with a Philips ESEM XL 30 scanning electron microscope equipped with an EDAX analyzer. X-ray powder patterns were recorded in transmission geometry using a STOE STADI P diffractometer (CuK_α = 1.54056 Å).

Syntheses of the complexes

$(pipH_2)[WS_4]$ (1). Ammonium tetrathiotungstate (348 mg, 1 mmol) was dissolved in distilled water (20 ml) and anhydrous piperazine (86 mg, 1 mmol) dissolved in distilled water (5 ml) was added at room temperature. The reaction mixture was stirred for ~ 5 min and then filtered. The clear filtrate was left undisturbed in a refrigerator. After 2 days yellow blocks of compound **1** were obtained. These were filtered, washed with ice-cold water (2 ml) followed by isopropanol (10 ml) and diethylether (10 ml), and dried under vacuum. Yield 80 %.
Elemental analysis found: C 12.18 (calc. 12.00), H 3.00 (3.03), N 7.03 (7.00), S 32.84 (32.04) %.

IR data: 2989, 2928, 2752, 2668, 1510, 1425, 1400, 1371, 1298, 1186, 1079, 909, 862, 556, 473 (ν_1), 454 (ν_3), 441, 267, 201, 191 (ν_4), 125, and 92 cm^{-1}.
Raman Data: 480 (ν_1), 460, 451 (ν_3), 438, 380, 203 (ν_2), and 183 (ν_4) cm^{-1}.
UV-Vis data in nm (ε_{max} in $mol^{-1}.l.cm^{-1}$) 393 (14800), 277 (18900), 221 (18600)

$(trenH_2)[WS_4]\cdot H_2O$ (2). The reaction of ammonium tetrathiotungstate (348 mg, 1 mmol) with tren (0.35 ml) in water (10 ml) instead of anhydrous piperazine in the earlier reaction resulted in the formation of compound **2** in 70 % yield.
Elemental analysis found: C 15.11 (calc. 15.06), H 4.72 (4.60), N 11.31 (11.63), S 26.23 (26.81) %.

IR data: 3471, 3330, 3278, 3084, 3009, 2886, 2829, 1601, 1569, 1513, 1478, 1345, 1295, 1142, 1086, 1007, 963, 857, 754, 481 (ν_1), 454 (ν_3), 357, 344, 247, 218, 203, 185 (ν_4), 133, and 101 cm^{-1}.
Raman data: 480, 467, 459 and 179 cm^{-1}.
UV-Vis data in nm (ε_{max} in $mol^{-1}.l.cm^{-1}$) 393 (16360), 277 (22460), 221 (23800).

Single crystal X-ray diffractometry

Intensity data were collected on a Philips PW1100-four circle diffractometer for **1** and AED2 four circle diffractometer for **2** at room temperature using graphite monochromated Mo-K_α radiation. For both compounds a numerical absorption correction was applied. The structures were solved with direct methods using

Table 5 Technical details of data acquisition and selected refinement results for $(pipH_2)[WS_4]$ **(1)** and $(trenH_2)[WS_4]\cdot H_2O$ **(2)**.

Compound	$(pipH_2)[WS_4]$ **1**	$(trenH_2)[WS_4]\cdot H_2O$ **2**
Formula	$C_4H_{12}WN_2S_4$	$C_6H_{22}N_4OWS_4$
MW /g/mol	400.25	478.37
Space group	$P2_1/c$	$P2_1/c$
a /Å	8.2534(7)	11.495(1)
b /Å	11.271(1)	11.810(1)
c /Å	11.996(1)	12.519(1)
β /°	95.11(1)	111.70(1)
Volume /Å^3	1111.6(2)	1579.2(2)
Z	4	4
Temperature / K	293	293
μ / mm^{-1}	11.09	7.83
F(000)	752	928
$D_{calc.}$ / g·cm^{-3}	2.392	2.012
2θ Range / °	3 − 60	3 − 60
hkl Range	0/11; −15/5; −16/16	−16/1; −16/16; −16/17
Refls. collected	4913	10399
Refls. unique	3241	4600
Data (Fo>4σ(Fo))	2632	3961
$R_{int.}$	0.0162	0.0193
Min./max. transm.	0.1631 0.3001	0.2413 / 0.3650
$\delta\rho$ /(e/Å^3)	−0.57 /0.58	−0.99 / 0.72
Parameters	101	146
$R1$ [Fo>4σ(Fo)]	0.0176	0.0170
$wR2$ for all data	0.0399	0.0401
Goodness of fit	0.990	1.062

Table 6 Atomic coordinates [·10^4] and equivalent isotropic displacement parameters [Å^2·10^3] for compounds **1** and **2**.

Atom	x	y	z	U_{eq}
$(pipH_2)[WS_4]$ (**1**)				
W(1)	7906(1)	2207(1)	5940(1)	22(1)
S(1)	10103(1)	3328(1)	6112(1)	30(1)
S(2)	5721(1)	3355(1)	5853(1)	30(1)
S(3)	7901(1)	1134(1)	4432(1)	34(1)
S(4)	7908(1)	1077(1)	7415(1)	30(1)
N(1)	4583(3)	2706(2)	3242(2)	28(1)
C(1)	3508(4)	3698(3)	2829(3)	32(1)
C(2)	2140(4)	3867(3)	3570(3)	34(1)
N(2)	1221(3)	2725(2)	3659(2)	28(1)
C(3)	2297(3)	1740(3)	4071(2)	30(1)
C(4)	3655(3)	1577(3)	3320(3)	30(1)
$(trenH_2)[WS_4]\cdot H_2O$ (**2**)				
W(1)	1790(1)	3573(1)	2326(1)	26(1)
S(1)	51(1)	3022(1)	2507(1)	41(1)
S(2)	1546(1)	3574(1)	502(1)	35(1)
S(3)	3272(1)	2415(1)	3301(1)	41(1)
S(4)	2255(1)	5302(1)	3006(1)	40(1)
N(1)	6402(2)	3910(2)	3076(2)	30(1)
C(1)	6720(2)	2725(2)	3419(2)	33(1)
C(2)	8027(2)	2642(2)	4321(2)	34(1)
N(2)	8368(2)	1437(2)	4633(2)	35(1)
C(3)	5935(2)	4492(2)	3881(2)	34(1)
C(4)	6274(3)	5729(2)	4001(2)	43(1)
N(3)	7648(2)	5873(2)	4462(2)	48(1)
C(5)	5490(2)	4003(2)	1890(2)	37(1)
C(6)	6027(3)	3708(2)	982(2)	39(1)
N(4)	7071(2)	4404(2)	974(2)	44(1)
O(1)	9402(3)	5450(2)	3447(3)	85(1)

Equivalent isotropic U calculated as a third of the trace of the orthogonalised U_{ij} tensors

SHELXS-97 [28] and refinement was carried out against F^2 using SHELXL-97 [29]. All non-hydrogen atoms were refined using anisotropic displacement parameters. The hydrogen atoms were located in difference maps but positioned with idealized geometry and refined using the riding model with fixed isotropic displacement parameters. The technical details of data acquisition and some selected refinement results are summarized in Table 5. The atomic coordinates and equivalent isotropic displacement parameters for compounds **1** and **2** are presented in Table 6.

Crystallographic data (excluding structure factors) have been deposited with the Cambridge Crystallographic Data Centre as supplementary publication no. CCDC 249579 (**1**) and CCDC 249578 (**2**). Copies of the data can be obtained, free of charge, on application to CCDC, 12 Union Road, Cambridge CB2 1 EZ, UK. (fax: +44-(0)1223-336033 or email: deposit@ccdc.cam.ac.uk).

Acknowledgements. Financial support by the State of Schleswig-Holstein and the Deutsche Forschungsgemeinschaft (DFG) is gratefully acknowledged. B.R.S. thanks the Department of Science and Technology (DST), New Delhi for financial support (SR/S1/IC-41/2003). W.B. and B.R.S. acknowledge the DST, New Delhi and Deutscher Akademischer Austauschdienst (DAAD) Bonn, for the sanction of a DST-DAAD (PPP) project.

References

[1] T. Rauchfuss, *Inorg. Chem*. **2004**, *43*, 14 and references cited therein.
[2] T. Shibhahara, *Coord. Chem. Rev*. **1993**, *123*, 73.
[3] D. Coucouvanis, *Adv. Inorg. Chem*. **1998**, *45*, 1.
[4] J. J. Berzelius, *Poggendorffs Ann. Phys. Lpz*. **1826**, *8*, 277.
[5] A. Müller, E. Diemann, R. Jostes, H. Bögge, *Angew. Chem.* **1981**, *93*, 957; *Angew. Chem. Int. Ed. Engl*. **1981**, *20*, 934 and references cited therein.
[6] A. Müller, E. Diemann, *Chem. Commun*. **1971**, 65.
[7] G. Alonso, G. Berhault, A. Aguilar, V. Collins, C. Ornelas, S. Fuentes, R. R. Chianelli, *J. Catal*. **2002**, *208*, 359.
[8] J. Ellermeier, R. Stähler, W. Bensch, *Acta Crystallogr*. **2002**, *C58*, m70.
[9] B. R. Srinivasan, S. N. Dhuri, C. Näther, W. Bensch, *Acta Crystallogr*. **2002**, *E58*, m622.
[10] B. R. Srinivasan, S. N. Dhuri, C. Näther, W. Bensch, *Acta Crystallogr*. **2003**, *C59*, m124.
[11] B. R. Srinivasan, S. N. Dhuri, C. Näther, W. Bensch, *Acta Crystallogr*. **2003**, *E59*, m681.
[12] B. R. Srinivasan, M. Poisot, C. Näther, W. Bensch, *Acta Crystallogr*. **2004**, *E60*, i136.
[13] J. Ellermeier, C. Näther, W. Bensch, *Acta Crystallogr*. **1999**, *C55*, 501.
[14] J. Ellermeier, C. Näther, W. Bensch, *Acta Crystallogr*. **1999**, *C55*, 1748.
[15] J. Ellermeier, W. Bensch, *Z. Naturforsch*. **2001**, *56b*, 611.
[16] J. Ellermeier, W. Bensch, *Monatsh. Chem*. **2002**, *133*, 945.
[17] B. R. Srinivasan, B. K. Vernekar, K. Nagarajan, *Indian J. Chem*. **2001**, *40A*, 563.
[18] B. R. Srinivasan, S. N. Dhuri, C. Näther, W. Bensch, *Inorg. Chim. Acta* **2005**, *358*, 279.
[19] J. Ellermeier, *Ph.D. thesis*, Christian-Albrecht Universität-Kiel, March 2002.
[20] I. Bezverkhyy, P. Afanasiev, M. Lacroix, *Mat. Res. Bull*. **2002**, *37*, 161.

[21] D. E. Schwarz, T. B. Rauchfuss, S. R. Wilson, *Inorg. Chem*. **2003**, *42*, 2410.
[22] B. R. Srinivasan, S. N. Dhuri, M. Poisot, C. Näther, W. Bensch, *Z. Naturforsch*. **2004**, *59b*, 1083.
[23] B. R. Srinivasan, C. Näther, W. Bensch, *Acta Crystallogr*. **2003**, *E59*, m639.
[24] B. R. Srinivasan, A. R. Naik, C. Näther, W. Bensch, *Acta Crystallogr*. **2004**, *E60*, m1384.
[25] J. W. McDonald, G. D. Friesen, L. D. Rosenhein, W. E. Newton, *Inorg. Chim. Acta* **1983**, *72*, 205.
[26] K. Nakamoto, *Infrared and Raman Spectra of Inorganic and Coordination Compounds*, 4th. Ed., John Wiley, New York, 1986, p. 130.
[27] T. P. Prasad, E. Diemann and A. Müller, *J. Inorg. Nucl. Chem*. **1973**, *35*, 1895.
[28] G. M. Sheldrick, *SHELXS-97, Program for the solution of crystal structures*, Univ. of Göttingen, Germany 1994.
[29] G. M. Sheldrick, *SHELXL-97, Program for the refinement of crystal structures*, Univ. of Göttingen 1997.

